Dependence of modulation bandwidth and chirp on carrier transport in high-speed quantum-well laser

MOUSTAFA AHMED
Department of Physics, Faculty of Science, King Abdulaziz University, 20203, Jeddah, Saudi Arabia

This paper investigates the impacts of the carrier transport processes in quantum well lasers on the modulation bandwidth and frequency chirp. The study is based on linearizing the rate equations using small-signal analysis. The major transport processes include carrier transport in the separate channel heterojunction (SCH) and escape in the well. We introduce analytical forms of the intensity modulation (IM) response and chirp to modulated power ratio. We show that when the transport process is fast and the escape process is slow, the bandwidth becomes highest, and Agrawal's relation of the bandwidth and resonance frequency applies. The chirp is independent of the transport processes.

(Received October 12, 2024; accepted April 15, 2025)

Keywords: Quantum well laser, Carrier transport, Small-signal analysis, Modulation

1. Introduction

QW lasers are preferential light sources in high-speed photonics because of their advantages of low-threshold current and high differential gain that results in high modulation bandwidth [1]. However, the modulation bandwidth and frequency chirp of QW lasers are affected by the carrier transport processes across the SCH layers due to diffusion time and capture of charge carriers, and in the well itself due to the thermionic emission, or equivalently the escape time from the well [1-4]. The transport time induces a low-frequency roll-off in the IM response [5-8], which manifests as a reduction of the modulation bandwidth. The bandwidth limitation was attributed to lower effective differential gain and a large K-factor [7]. The K-factor, also known as "Petermann's factor", is a measure of how much the laser linewidth is broadened compared to the classical Schawlow-Townes linewidth formula [8]. Therefore, the carrier transport times should be controlled to increase the bandwidth [10]. On the other hand, because of the fairly small optical confinement factors in QW laser, the carrier density variations add to the frequency chirp [11-15]. The transport processes across the SCH and QW layers were reported to influence both the efficiency and the shape of frequency modulation [16-19]. The frequency chirp should be reduced for an efficient application of QW lasers, for instance, in fiber links to minimize the fiber dispersion effect [20]. The chirp-to-modulated power ratio (CPR) is an efficient quantity to assess the frequency chirp accompanying the intensity modulation [21]. Therefore, the control and reduction of the frequency chirp in QW lasers require addressing the dependence of CPR on the transport processes in the QW structure. There were minor reports in the literature that discuss the impacts of the carrier transport process on the frequency chirp [11-14], in general, and on CPR [22], in particular.

Simulation of the intensity modulation properties of QW lasers and the associated modulated chirp is analyzed by numerical integration of three rate equations that describe the time evolution of the photon density emitted in the active region and carrier densities in both the QW and barrier [7]. Very recently, the authors have introduced modeling of the IM response in QW lasers based on linearizing the rate equations of the QW laser using the small–signal approximation [23]. The individual impacts of the escape and capture times on the IM response were elucidated. However, the transport processes in the SCH layer were limited only to the capture of carriers by the QW, and hypothetical wide ranges of values were assumed for the escape and capture times, which could make the carrier density in the barrier greater than that in the QW.

In this work, we extend the theoretical model in [23] to account for the frequency chirp associated with the intensity modulation of the QW lasers. We investigate dependencies of the modulation bandwidth and CPR on the transport processes in the SCH and QW layers using realistic values of the corresponding transport times. The transport processes in the SCH layer include both the capture of carriers by the QW and the diffusion across the SCH itself. Analytic forms are derived for the IM response and frequency chirp CPR. We use the calculated results to investigate how the modulation bandwidth f_{3dB} of the laser is related to its relaxation frequency f_r, a relation of practical importance, and compare it with the famous Agrawal's relationship $f_{3dB} = \sqrt{3} f_r$. The results indicate that the modulation bandwidth becomes maximum when the escape process is so relaxed with a rather long escape time and the carrier diffusion in the SCH layer is so fast that the transport time is very short. The increase of the escape time could be achived by by icreasig the thickness of the QW [24], while the reduction of transport time could be realized by shorteing the SCH layer [25,26]. Over these ranges, CPR at the peak frequency becomes highest and the Agrawal equation of f_{3dB} and f_r fits well. Shortening the escape time limits the bandwidth, reducing CPR, and deviation from Agrawal's equation. The findings in this study advance and supplement the theory and simulation of QW laser diodes.

2. Theoretical model

In the current SCH-QW model, charge neutrality is assumed to hold in the entire intrinsic SCH region. The exterior edges of the left and right SCH regions are used to inject charge carriers into the QW. Before recombination by stimulated emission, the injected carriers diffuse into the SCH region and are captured in the QW [27]. In addition, thermionic emission works against carrier capture and reduces the QW structure's total carrier capture efficiency [28]. The carrier transport across the SCH is characterized by the ambipolar diffusion time τ_{diff} and the capture time τ_{cap} in the QW, $\tau_{SCH} = \tau_{diff} + \tau_{cap}$ [25,26]. The diffusion time is determined by the thickness L_{SCH} of the SCH layer and the ambipolar diffusion coefficient D_a. The carrier capture time τ_{cap} is the duration of capturing carriers from the SCH states to the QW states. According to R. Nagarajan et al. [1], the local carrier capture time at the QW is smaller than 1 ps for both the electrons and the holes. In the GaAs-AlGaAs laser system, the quantum carrier capture time was reported to be 0.65ps for the holes and 1.2ps for the electrons independent of quantum-well width [24]**.** The carrier escape (or thermionic emission) τ_{esc} is the time the carriers take to escape from the QW states to the SCH layer states and is proportional to the thickness L_w of the QW [29].

The rate equations that describe the evolution of the carrier number $N(t)$ and photon number $S(t)$ in the QW, optical phase $\theta(t)$, and carrier number $N_{SCH}(t)$ in the SCH or barrier layer are [30]:

$$\frac{dS}{dt} = \Gamma G(N,S)S - \frac{S}{\tau_p} + \beta_{sp}\frac{N}{\tau_e} \tag{1}$$

$$\frac{dN}{dt} = \frac{N_{SCH}}{\tau_{SCH}} - \frac{N}{\tau_{esc}} - \frac{N}{\tau_e} - G(N,S)S \tag{2}$$

$$\frac{dN_{SCH}}{dt} = \frac{1}{e}(I_b + I_m \sin 2\pi f_m t) + \frac{N}{\tau_{esc}} - \frac{N_{SCH}}{\tau_{SCH}} \tag{3}$$

$$\frac{d\theta}{dt} = \frac{1}{2\pi}\Delta\nu(t) = \frac{1}{2\pi}\left[\nu - \nu_0 + \frac{\alpha}{2}\left(\Gamma G(N,S) - \frac{1}{\tau_p}\right)\right] \tag{4}$$

The first and last terms of equation (1) describe the addition of photons due to the stimulated and spontaneous emission, respectively, while the second term corresponds to the rate of loss of photons due to the total loss in the laser region. τ_p is the photon lifetime, β_{sp} is the spontaneous emission factor, and Γ is the confinement factor in the QW. The function $G(N,S)$ defines the optical gain and is defined in this paper as [31]

$$G(N.S) = \frac{\frac{g_0}{V}(N-N_g)}{1+\varepsilon S} \tag{5}$$

where $\frac{g_0}{V}(N - N_g)$ represents the linear gain, where g_0 is the slope gain coefficient, and N_g is the carrier density at transparency. Equation (2) describes the rate of adding carriers to the QW due to carrier transport from the SCH layer, which is characterized by the transport lifetime τ_{SCH}, (first term), and the rate of carrier loss due to carrier escape from the QW (second term) characterized by lifetime τ_{esc}, and rates of carrier loss due to spontaneous and stimulated emission (third and fourth terms), respectively. In this equation, τ_e defines the spontaneous emission lifetime. The first term of equation (3) concerns the rate of carrier supply with a bias component I_b and a sinusoidal modulation component of amplitude I_m and frequency f_m, while the second and third terms describe the rate of add and drop of charge carrier in the SCH layer through the transport and escape processes in the SCH layer and QW, respectively. In equation (4), $\Delta\nu(t)$ is the frequency chirp, ν is the frequency of the oscillating mode, ν_o is the frequency of the cold mode in the laser resonator, and α is the linewidth enhancement facor.

The above rate equations are linearized for the case of small-signal modulation that corresponds $I(t) = I_b + \Delta I_m(t)$ with the modulation component ΔI_m << I_b,. The gain is expanded by the Taylor expansion around the bias values N_b and S_b up to the second term as

$$G(N,S) = G_b(N_b,S_b) + \frac{\partial G}{\partial N}\Delta N + \frac{\partial G}{\partial S}\Delta S \tag{6}$$

By applying the Fourier transformation of the modulation amplitude:

$$\Delta X(t) = \int_{-\infty}^{\infty} X_m e^{j\Omega_m t} d\Omega_m \tag{7}$$

where X_m applies for the modulation amplitudes I_m, S_m, N_m, N_{SCHm}, and $\Delta\nu_m$, and $\Omega_m = 2\pi f_m$ is the angular frequency, the following equations of the modulation components are derived:

$$\left(j\Omega_m + \frac{\varepsilon\Gamma S_b}{1+\varepsilon S_b}G_b\right)S_m - \left(\frac{\Gamma\frac{g_0}{V}S_b}{1+\varepsilon S_b}\right)N_m = 0 \tag{8}$$

$$\left[j\Omega_m + \left(\frac{1}{\tau_{esc}} + \frac{1}{\tau_e} + \frac{\frac{g_0}{V}S_b}{1+\varepsilon S_b}\right)\right]N_m + \left[\left(1 - \frac{\varepsilon S_b}{1+\varepsilon S_b}\right)G_b\right]S_m - \left(\frac{1}{\tau_{SCH}}\right)N_{SCHm} = 0 \tag{9}$$

$$\left(j\Omega_m + \frac{1}{\tau_{SCH}}\right) N_{SCHm} - \left(\frac{1}{\tau_{esc}}\right) N_m = \frac{I_m}{e} \quad (10)$$

$$\Delta\nu_m = \frac{\alpha}{4\pi} \frac{\Gamma \frac{g_0}{V}}{1+\varepsilon S_b} N_m \quad (11)$$

The steady-state components of *S*, *N*, and N_{SCH} and the chirp are determined from the equations:

$$S_b = \frac{\Gamma\tau_p}{e}(I_b - I_{th}) \quad (12)$$

$$N_b = \frac{\frac{I}{e}(1+\epsilon S_b) + g_0 N_g S_b}{\frac{1}{\tau_e}(1+\epsilon S_b) + g_0 S_b} \quad (13)$$

$$N_{SCHb} = \tau_{SCH}\left(I_b + \frac{N_b}{\tau_{esc}}\right) \quad (14)$$

$$\Delta\nu_b = \frac{\alpha}{4\pi}\left(\Gamma G_b - \frac{1}{\tau_p}\right) \quad (15)$$

According to equation (14), the values of τ_{SCH} should not exceed the values of τ_{esc} to keep the injected carrier number in the barrier smaller than the carrier number in the QW. After tedious mathematical derivation ignoring the spontaneous emission, the IM response and the chirp-to-power ratio (CPR) at a specific bias current I_b and modulation frequency Ω_m can be proved to be:

$$IM(\Omega_m) = \frac{S_m(\Omega_m)}{S_m(\Omega_m \to 0)} = \frac{\Omega_C^3}{-j\Omega_m(\Omega_m^2 - \Omega_B^2) - \Omega_A\Omega_m^2 + \Omega_C^3} \quad (16)$$

$$CPR(\Omega_m) = \frac{\Delta\nu_m}{P_m} = \frac{\alpha}{4\pi P_b S_b}\left(j\Omega_m + \frac{\Gamma\varepsilon S_b}{1+\varepsilon S_b} G_b\right) \quad (17)$$

where the frequency components Ω_A, Ω_B^2, and Ω_C^3 are given by

$$\Omega_A = \frac{1}{\tau_e} + \frac{1}{\tau_{esc}} + \frac{1}{\tau_{SCH}} + \frac{S_b}{1+\varepsilon S_b}\left(\frac{g_0}{V} + \Gamma\varepsilon G_b\right) \quad (18)$$

$$\Omega_B^2 = \frac{1}{\tau_e\tau_{SCH}} + \frac{S_b}{1+\varepsilon S_b}\left[\frac{g_0}{V}\left(\frac{1}{\tau_p} + \frac{1}{\tau_{SCH}}\right) + \Gamma\varepsilon G_b\left(\frac{1}{\tau_e} + \frac{1}{\tau_{SCH}} + \frac{1}{\tau_{esc}}\right)\right] \quad (19)$$

$$\Omega_C^3 = \frac{S_b}{1+\varepsilon S_b}\left(\frac{g_0}{V}\frac{1}{\tau_p} + \frac{\Gamma\varepsilon G_b}{\tau_e}\right) \quad (20)$$

The bandwidth is determined as the 3dB frequency f_{3dB}, or the frequency at which the IM response $|IM(\Omega)|$ drops to one-half of its value $|IM(\Omega_m \to 0)|$. The chirp CPR is a significant figure-of-merit for the chirp.

3. Results and discussion

In this paper, we apply the present small-signal model to investigate the influence of the carrier transport effects on the IM response, modulation bandwidth, and frequency chirp.

The first step is to calculate the steady-state components *S*, *N*, and N_{SCH} using equations (12) – (14), respectively, at the given input parameters, including the bias current I_b, transport time τ_{SCH} and escape time τ_{esc}. Then equations (16) and (17) are applied to calculate modulation response IM(Ω_m) and chirp CPR(Ω_m) vias equations (16) and (17), respectively. We used the Matchad-15 software to perform such calculations. Table 1 lists the numerical values used in the calculations, which correspond to 1.55μm-InGaAsP QW lasers [30]. The corresponding threshold current of the QW laser under investigation is I_{th} = 63 mA. Ranges of values are set for τ_{SCH} and τ_{esc} that correspond to varied values of the SCH and QW thicknesses. The values of τ_{SCH} should not exceed the values of τ_{esc} to keep the injected carrier number in the barrier N_b smaller than the carrier number *N* in the QW.

Table 1. Numerical values of the QW laser under investigation [23]

Symbol	Definitions of parameters	Value
λ	Wavelength	1550 nm
V	Active layer volume	7.2×10^{-18} m^3
g_o	slope gain coefficient	$1.925\text{x}10^{-11}$
N_o	Carrier number at	8.21×10^6
Γ	Mode confinement factor	0.088
τ_e	Carrier lifetime	0.3 ns
τ_p	Photon lifetime	1.2 ps
β	Spontaneous emission	3×10^{-5}
ε	Gain compression	2×10^{-7}

3.1. Influence of carrier transport on modulation characteristics

Fig. 1(a) plots the frequency spectra of the IM response for three sets of the SCH transport time and escape time; namely, τ_{SCH} = 10ps & τ_{esc} = 10ps, τ_{SCH} = 1ps & τ_{esc} = 10ps, and τ_{SCH} = 10ps & τ_{esc} = 100ps. The bias current is $I_b = 2I_{th}$. For the three cases, the figure shows that the response is flat in the regime of low modulation frequencies and increases in the regime of high frequencies attaining a maximum value at peak frequency, which is nearly equal to the relaxation frequency of the laser. Then the IM response declines to much lower values beyond the IM response peak reaching a value of 3dB at the modulation bandwidth f_{3dB}. When τ_{SCH} = 10ps & τ_{esc} = 10ps, the characteristic frequencies are f_{peak} = 8.3GHz and f_{3dB} = 14.14GHz. The figure shows that these frequencies increase with the decrease of the SCH transport time to τ_{SCH} = 1ps (f_{peak} = 9.61GHz and f_{3dB} = 16.42GHz) or the increase of the escape time to τ_{esc} = 100ps (f_{peak} = 11.55GHz and f_{3dB} = 17.8GHz).

The former corresponds to a faster carrier transport process through the SCH layer, while the second corresponds to a slower carrier escape from the QW.

The corresponding frequency variation of the chirp to modulated power ratio, CPR, which evaluates the amount of variation of the lasing frequency associated with or induced by the intensity modulation, is plotted in Fig. 1(b).

As shown in the figure, the CPR increases almost linearly with the increase of the modulation frequency, as inferred from equation (17), and is independent of the value of either τ_{SCH} or τ_{esc}.

That is, the carrier transport processes have a remarkable impact on the IM response, including the peak frequency f_{peak} and bandwidth f_{3dB}, whereas they do not affect the chirp to modulated power ratio CPR.

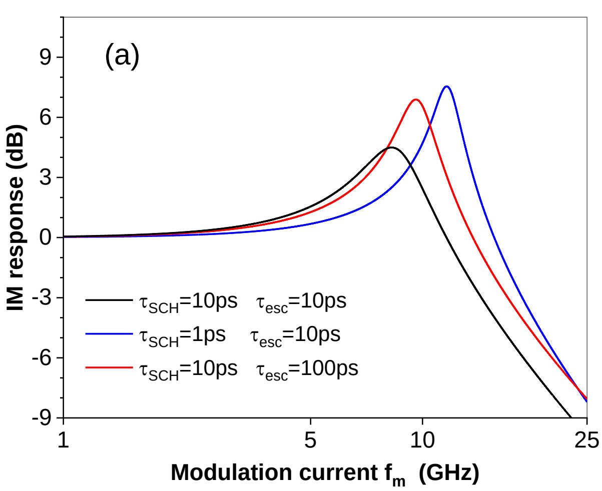

Fig. 1. Plot of the spectrum of (a) IM response, and (b) chirp CPR, when τ_{SCH} = 10ps ad τ_{esc} = 100ps (colour online)

Now we examine the dependence of the modulation bandwidth and chirp CPR on both τ_{esc} and τ_{SCH}. Fig. 2 plots the variation of the bandwidth f_{3dB} with τ_{SCH} at different values of τ_{esc} ranging between 10 and 100ps. The transport time varies up to the value of the escape time τ_{esc} to keep the injected carrier number in the barrier smaller than the carrier number in the QW. The figure shows that the largest value of f_{3dB} = 26.1GHz is predicted at the shortest time τ_{SCH} =1ps and longest time τ_{esc} =100ps. However, an increased escape time is generally associated with a thicker quantum well, resulting in slower carrier transport, reduced current flow, and potentially diminished device performance in terms of speed and efficiency. Therefore, a trade-off must be established between escape time and faster carrier transport to optimize the performance of high-efficiency lasing devices, while avoiding extreme, unreliable operating conditions. The increase of τ_{SCH} lowers the bandwidth up to values between 16 and 18GHz, depending on the value of τ_{esc}. The decrease of τ_{esc} is seen to cause much reduction of f_{3dB}. The bandwidth reduction can be attributed to the increase of the carrier number N_{Bb} in the SCH layer which relaxes the lasing action in the QW.

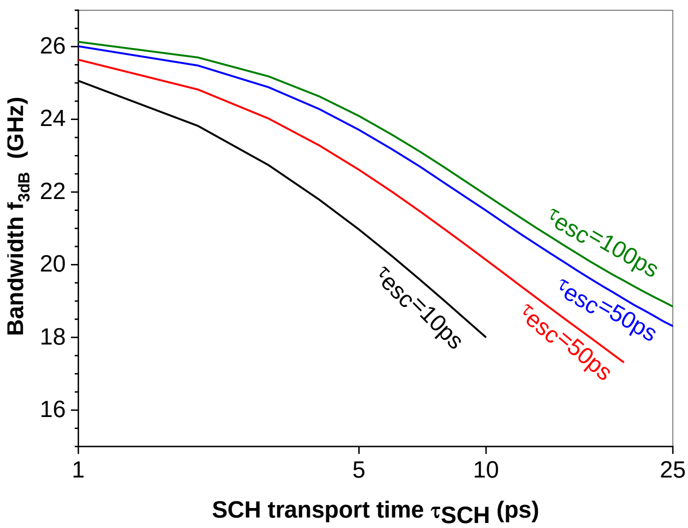

Fig. 2. Variation of the bandwidth f_{3dB} with τ_{SCH} at different values of the escape time τ_{esc}. The bias current is I_b=3I_{th} (colour online)

In Fig. 3, the values of the chirp to power ratio CPR_{peak} calculated at the peak frequency of the QW laser are plotted, respectively, over the entire ranges of τ_{esc} and τ_{SCH} in Fig. 3. The figure indicates that CPR_{peak} varies between 5 and 46 GHz/mW. CPR_{peak} changes with the lifetimes almost in a similar fashion to the bandwidth f_{3dB} in Fig. 2. CPR_{peak} decreases with the increase of τ_{SCH} but increases with the increase of τ_{esc} up to τ_{SCH}=20ps. τ_{SCH}>20ps, CPR_{peak} is almost constant independent of the value of τ_{esc}. That is, the chirp values increase almost in a similar fashion to the bandwidth, and the decrease of carrier transport times τ_{esc} and τ_{SCH} work to lower the frequency chirp associated with the intensity modulation for the laser.

It is worth noting that the change of CPR_{peak} with both τ_{SCH} and τ_{esc} despite the independence of CPR of τ_{SCH} and τ_{esc} in equation (17) is attributed to the change of the peak frequency f_{peak}, as indicated in Fig. 1(b).

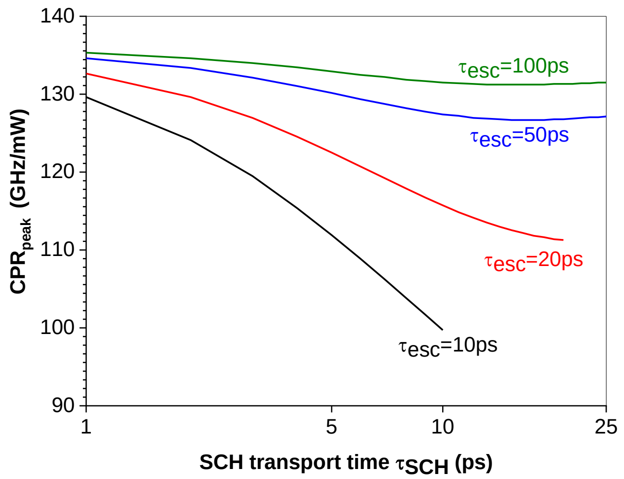

Fig. 3. Plot of frequency chirp per power ratio CPR_{peak} versus the transport time τ_{SCH} at different values of the escape time τ_{esc} (colour online)

3.2. Influence of bias current on modulation performance

The influence of I_b on the bandwidth f_{3dB} is illustrated in Fig. 4(a) for three values of τ_{SCH} = 1, 5, 10, and 20ps when τ_{esc} = 100ps). The figure shows that for the different values of the transport time τ_{SCH}, f_{3dB} increases with the increase of I_b, and this increase is parabolic as the common feature of semiconductor lasers [32-34]. This behavior was recorded in experiments of Nagarajan et al. [7] who reported an increase of f_{3dB} by an amount of 15GHz and the peak frequency f_{peak} by 14GHz of an InGaAs QW laser with the increase of 20mW power, Grabmaier et al. [35] of the increase of f_{3dB} by an amount of 38GHz of a 1.55-µm DFB QW laser with the increase of 9mW power, Wsiak et al. [36] of the increase of f_{3dB} by an amount of 20GHz and f_{peak} by 14GHz of a GaAs-based VCSEL with the increase of current of 4mA, and Keating et al. [37] of an increase of f_{3dB} by 4GHz and f_{peak} by 2.2GHz of a 1.55-µm DFB QW laser with the increase of current of 18mA. It is worth noting that Fig. 4(a) also indicates a reduction in the bandwidth frequency f_{3dB} associated with the increase in τ_{SCH}. When τ_{SCH}=1ps, f_{3dB} increases from 5 to 50GHz with the current increase from 1.1 to 5 times I_{th}, while they increase from 5 to 34 GHz when the transport time increases to 20ps.

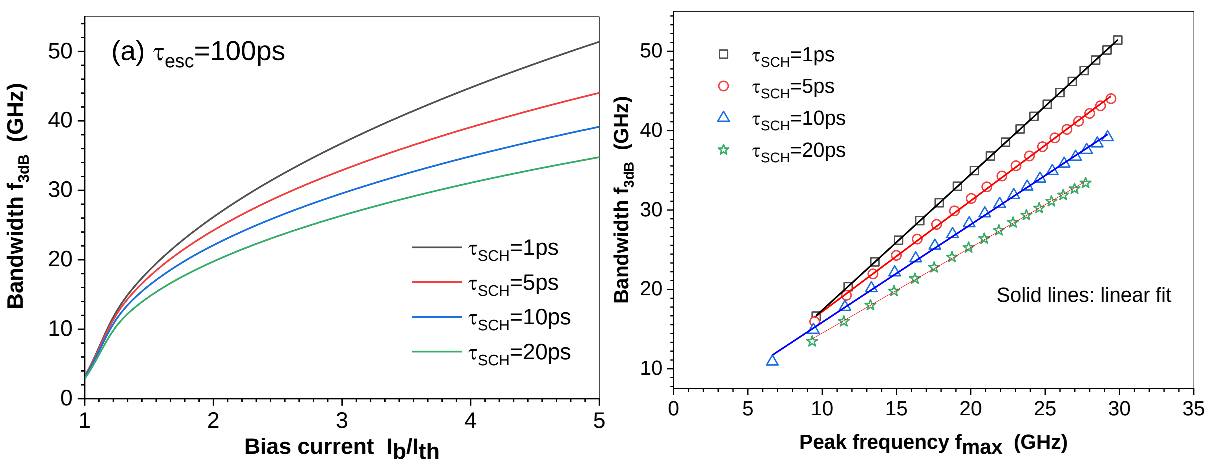

Fig. 4. Plot of (a) Variation of the modulation bandwidth f_{3dB} with bias current, and (b) relationship between f_{3dB} and f_{peak}, when τ_{SCH} = 1,5, 10 and 20ps with τ_{esc} = 20ps

Based on theoretical modeling of the intensity modulation of the semiconductor laser, Agrawal et al. [32] reported that the modulation bandwidth is related to the peak frequency as $f_{3dB} = \sqrt{3} f_{peak}$. It is interesting to examine the validity of this relationship in the current case of QW laser from the data given in Fig. 4(a). Fig. 4(b) plots f_{3dB}versus f_{peak} at the different values of the transport time τ_{SCH}. The figure indicates that the relation between $f_{3dB}$and f_{peak} is linear for the different values of τ_{SCH}, as indicated by the linear fitting of $f_{3dB} = f_{3dB0} + mf_{peak}$, where f_{3dB0} if the intercept of the f_{3dB}-axis and m is the slope. Table 2 lists the values of f_{3dB0} and m calculated for different values of τ_{SCH}, and indicates that the slope m decreases while the intercept f_{3dB0} increases with the increase of τ_{SCH}. The values of m and f_{3dB0} closest to those of the Agrawal's relation correspond to the shortest transport time τ_{SCH} = 1ps. That is, the famous Agrawal's relation between f_{3dB}versus f_{peak} works well when the transport process is too fast and the escape process is too slow.

The corresponding impact of current on the frequency chirp to current ratio CPR_{peak} calculated at the peak frequency f_{peak} is depicted in Fig. 5. The figure shows that the chirp values are reduced with the increase of current I_b, and this reduction is remarkable in the region of low currents. As a numeric example, CPR_{peak} = 194GHz/mW when I_b = 1.1I_{th}, which is much reduced to CPR_{peak} = 75GHz/mW when I_b = 5.0I_{th}. These reductions of the chirp values are then associated with the improvement of the laser coherency with the increase of the bias current I_b. The figure indicates that CPR_{peak} is insensitive to the carrier transport processes.

Table 2. Values of the fitting parameters m and f_{3dB0} of the relationship between f_{3dB} and f_{peak}

τ_{SCH}	Intercept frequency f_0 (GHz)	Slope m
1ps	0.255	1.71
5ps	3.226	1.40
10ps	3.52	1.232
20ps	3.71	1.08

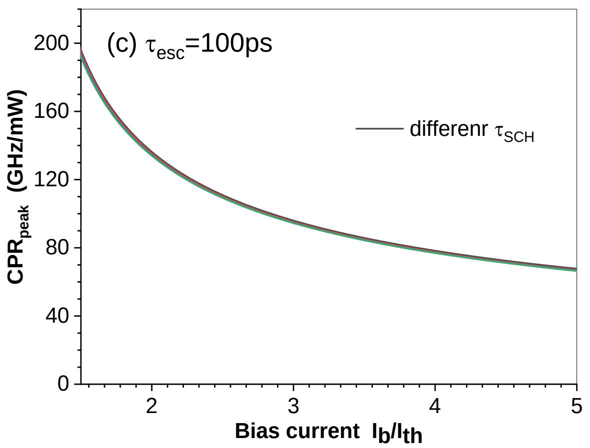

Fig. 5. Plot of the frequency chirp to power ratio CPR_{peak} versus the bias current I_b when τ_{SCH} = 1, 5, 10 and 20ps with τ_{esc} = 100ps

4. Conclusions

The transport and diffusion processes of the charge carriers in the QW structure have significant impacts on the modulation bandwidth and the frequency chirp of QW laser under direct current modulation. By applying the small signal analysis and characterizing the transport process in the SCH layer and the escape process in the well by the corresponding lifetimes τ_{SCH} and τ_{cap}, respectively, the present work leads to the following conclusions. When the escape process is as slow as τ_{esc} = 100ps, the longer the SCH transport time τ_{SCH}, the lower the bandwidth and frequency chirp. When τ_{esc} = 10ps, the decrease of τ_{SCH} is associated with shifting the bandwidth f_{3dB} towards higher frequencies and an increase in the peak frequency. CPR increases linearly with the increase in the modulation frequency and is independent of the values of τ_{SCH} and τ_{esc}. The largest value of f_{3dB} = 26.1GHz is predicted at the shortest time τ_{SCH} = 1ps and longest time τ_{esc} =100ps. The increase of τ_{SCH} results in lowering the bandwidth up to values between 16 and 18GHz, depending on the value of τ_{esc}. The values of CPR_{peak} vary between 5 and 46 GHz/mW. These chirp values increase almost in a similar fashion to the bandwidth and decrease with the increase of τ_{esc} and τ_{SCH} due to the corresponding change in the peak frequency. The increase of the bias current at a given transport time results in an increase of f_{3dB} and a decrease in the chirp CPR_{peak}, and these variations are parabolic. The famous Agrawal's relation relating the 3dB-bandwidth to the resonance frequency, $f_{3dB} = \sqrt{3}f_{peak}$, of semiconductor lasers works well when the transport process is too fast and the escape process is too slow. Over the relevant range of the bias current, CPR_{peak} is insensitive to the carrier transport processes.

References

[1] R. Nagarajan, M. Ishikawa, T. Fukushima, R. S. Geels J. E. Bowers, IEEE J. Quantum Electron. **28**(10), 1990 (1992).
[2] M. O. Vassell, W. F. Sharfin, W. C. Rideout, J. Lee, IEEE J. Quantum. Electron. **29**(5), 1319 (1993).
[3] S. C. Kan, D. Vassilovski, T.C. Wu, K.Y. Lau, IEEE Photon. Technol. Lett. **4**(5), 428 (1992).
[4] S. C. Kan, D. Vassilovski, T. C. Wu, K. Y. Lau, Appl. Phys. Lett. **61**, 752 (1992).
[5] W. Rideout, W. F. Sharfin, E. S. Koteles, M. O. Vassell, B. Elman, IEEE Photon. Technol. Lett. **3**(9), 784 (1991).
[6] R. Nagarajan, T. Fukushima, S. W. Corzine, J. E. Bowers, Appl. Phys. Lett. **59**(15), 1835 (1991).
[7] R. Nagarajan, T. Fukushima, M. Ishikawa, J. E. Bowers, R. S. Geels, L. A. Coldren, IEEE Photon. Technol. Lett. **4**(2), 121 (1992).
[8] M. E. Mashade, J. Arnaud, IEEE J. Quantum Electron. **22**(4), 505 (1986).
[9] M. Homar, C. R. Mirasso, I. Esquivias, M. San Miguel, IEEE Photon. Technol. Lett. **8**(7),

861 (1996).
[10] R. Nagarajan, T. Fukushima, J. E. Bowers, R. S. Geels, L. A. Coldren, Appl. Phys. Lett. **58**(15), 2326 (1991).
[11] R. Ribeiro, J. da Rocha, A. Cartaxo, H. da Silva, B. Franz, B. Wedding, IEEE Photon. Technol. Lett. **7**(8), 857 (1995).
[12] E. Peral, W. Marshall, A. Yariv, J. Lighwave Technol. Lett. **16**(10), 1874 (1998).
[13] E. Peral, A. Yariv, IEEE Photon. Technol. Lett. **11**(3), 307 (1999).
[14] O. Nobuyuki, K. Masahiro, I. Masato, M. Yasushi, IEEE J. Quantum Electron. **32**(7), 1230 (1996).
[15] P. Krehlik, Adv. Electron. Telecommun. **1**(2), 63 (2010).
[16] A. P. Wright, B. Carrett, G. Thompson, J. Whiteaway, Electron. Lett. **28**(2), 1911 (1992).
[17] H. Yd. M. Yamagwhi, M. Kitamura, I. Mito, IEEE Photon. Technol. Lett. **5**(4), 396 (1993).
[18] R. Nagarajan, J. E. Bowers, IEEE J. Quantum Electron. **29**(6), 1601 (1993).
[19] R. F. S. Ribeiro, J. R. F. da Rocha, A. V. T. Cartaxo, H. J. A. da Silva, B. Franz, B. Wedding, IEEE Photonics Lett. **7**(8), 857 (1995).
[20] G. P. Agrawal, Fiber-Optic Communication Systems, John Wiley and Sons, Inc., New York, Ch. 2, 2002.
[21] O. Doyle, P. B. Gallion, IEEE J. Quantum Electron. **24**(3), 516 (1988).
[22] J. He, IEEE Photon. Technol. Lett. **19**(5), 285 (2007).
[23] M. Ahmed, M. Al-Alhumaidi, J. Comput. Electron. **22**(6), 1140 (2023).
[24] S. Morin, B. Deveaud, F. Clerot, K. Fujiwara, K. Mitsunaga, IEEE J. Quantum Electron. **27**(6), 1669 (1991).
[25] G. Eisenstein, J. M. Wiesenfeld, M. Wegener, G. Sucha, D. **S.** Chemla, S. Weiss, G. Raybon, U. Koren, Appl. Phys. Lett. **58**(2), 158 (1991).
[26] S. Weiss, J. M. Wiesenfeld, D. **S.** Chemla, G. Raybon, G. Sucha, M. Wegener, G. Eisenstein, C. A. Bums, A. G. Dentai, U. Koren, B. I. Miller, H. Temkin, R. A. Logan, T. Tanbun-Ek, Appl. Phys. Lett. **60**(1), 9 (1992).
[27] A. G. Plyavenek, Opt. Commun. **113**(1-3), 259 (1994).
[28] R. Nagarajan, T. Fukushima, J. E. Bowers, R. S. Geels, L. A. Coldren, Electron. Lett. **27**, 1058 (1991).
[29] H. Schneider, K. V. Klitzing, Phys. Rev. B **38**(9), 6160 (1988).
[30] R. N. Hall, G. E. Fenner, J. D. Kingsley, T. J. Soltys, R. O. Carlson, Phys. Review Lett. **9**(9), 366 (1962).
[31] M. Ahmed, M. Yamada, J. Appl. Phys. **84**(6), 3004 (1998).
[32] G. P. Agrawal, IEEE J. Quantum Electron. **26**(11), 1901 (1990)
[33] M. Ahmed, A. Bakry, R. Altuwirqi, M. S. Alghamdi, F. Koyama, Jap. J. Appl. Phys. **53**, 124103 (2013).
[34] M. S. Al-Ghamdi, H. Dalir, A. Bakry, M. Ahmed, Jap. J. Appl. Phys. **58**, 112003 (2019).
[35] A. Grabmaier, M. Schiifthaler, A. Hangleiter, Appl. Phys. Lett. **62**(1), 52 (1993).
[36] M. Wasiak, P. Spiewak, N. Haghighi, M. Gebski, E. P. Karbownik, P. Komar, J. A. Lott, R. P. Sarzała, J. Phys. D **53**(34), 345101 (2020).
[37] T. Keating, X. Jin, S. L. Chuang, K. Hess, IEEE J. Quantum Electron. **35**(10), 1526 (1999).

*Corresponding author: mhafidh@kau.edu.sa